A Comparative Study Using Small-Angle X-ray Scattering and Solid-State NMR of Microdomain Structures in Poly(styrene−butadiene−styrene) Triblock Copolymers

Hongshi Yu,[†] Almeria Natansohn,*[,†] Marsha A. Singh,[‡] and Tomas Plivelíc[§]

Department of Chemistry, Queen's University, Kingston, Ontario, Canada K7L 3N6; Department of Physics, Queen's University, Kingston, Ontario, Canada K7L 3N6; and National Synchrotron Light Laboratory (LNLS)/CNPq, Campinas, SP, Brazil

Received June 30, 1999; Revised Manuscript Received August 21, 1999

ABSTRACT: The complementary techniques of solid-state NMR and small-angle X-ray scattering (SAXS) have been used to determine the microdomain structures of a series of commercial poly(styrene-*b*-butadiene-*b*-styrene) triblock copolymers with different molecular weights. The relative locations of multiple scattering peaks, indirect transform, and Porod analysis have been used to determine the morphology and the sizes of various domains as well as the interfacial thickness between them. Solid-state NMR of ^{1}H spin diffusion measurements was also used to estimate the microdomain structure parameters by simulating the spin diffusion processes with a model that considers the effects of ^{1}H spin−lattice relaxation. The interfacial thickness, 2 nm for all five materials, and the interdomain distances, ranging from 30 to 42 nm, from NMR agree well with results from SAXS techniques. There are some discrepancies for some of samples regarding the domain sizes of dispersed polystyrene phases obtained from the above two techniques. These discrepancies may be mainly caused by the limited quality of the fitting procedure using indirect transform methods.

1. Introduction

Microphase separation in a two-component block copolymer is a well-known phenomenon in which the two different components form different ordered microdomains. One class of block copolymers, thermoplastic elastomers, has attracted much attention because of its quite useful properties. These thermoplastic elastomers are phase-separated materials, consisting of a dominant rubber phase and a dispersed rigid polystyrene phase. The dispersed polystyrene blocks form hard domains within the elastomer matrix and act as physical cross-links. These cross-links give the material its high tensile strength while the rubber blocks give its elasticity. The properties of materials are strongly related to the morphology, the sizes of domains, and the interfacial thickness of the materials.

A variety of techniques, such as thermal analysis, relaxation, microscopy, spectroscopy, scattering, and computer simulation, are available to probe the heterogeneity of multiphase systems. Each method has its own advantages and disadvantages. With increasing demands on the control of the properties of advanced materials, improvements of the characterization tools are needed. Solid-state NMR has been proven to be a very powerful method for characterizing the microdomain structures in various polymer systems, such as polymer blends[1−5] and block polymers.[6−10] The spin−lattice relaxation time in the laboratory [T_1(H)] and rotating frame [$T_{1\rho}$(H)] can be used as probes to identify the heterogeneity of the materials at different levels, and the actual values can be used to estimate the lower and/or upper limits of the domain sizes. The two-dimensional heteronuclear wide-line separation (WISE) technique can be used to establish a correlation between the microphase structure and segmental mobility in the probed system. In addition, various spin diffusion techniques have been used to quantify the sizes of each domain and the interface between the domains. Spin diffusion is a spatial diffusion of nuclear magnetization mediated by dipolar couplings normally without material transport. This process is distinct from a process involving mass transport of atoms in the sample, which might also cause a diffusion of nuclear magnetization. The experiment contains three steps: an initial pulse destroys the magnetization of one component and leaves the magnetization of the other component as a magnetization source. In the following mixing time, the magnetization can redistribute in space by "spin diffusion". The integral distribution of the magnetization in the spectrum is then detected for varying mixing times. The microscopic dimensions of the polymer domains can be extracted from computer simulation of the NMR signal intensities as a function of mixing time in the spin diffusion experiments.

The major advantages of this method are the very high resolution and its generality of application. The detectable domain sizes range from nanometers to hundreds of nanometers. Because of its high resolution, it is very useful for interface studies. Recently, there has been increased interest in the interfacial structure of heterogeneous polymer systems from both theoretical and experimental points of view. Small-angle X-ray scattering (SAXS) and small-angle neutron scattering (SANS) techniques have proven useful to estimate the thickness of interface in previous studies. The resolution of more standard techniques such as scanning electron microscopy (SEM) and transmission electron microscopy

[†] Department of Chemistry, Queen's University.
[‡] Department of Physics, Queen's University.
[§] National Synchrotron Light Laboratory.
* Corresponding author.

10.1021/ma9910585 CCC: $18.00
Published on Web 10/02/1999

Scheme 1. Chemical Structure of the SBS Samples

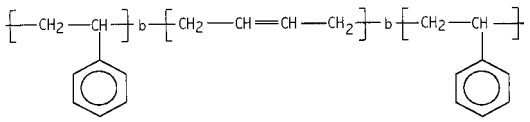

polystyrene, cis and trans polybutadiene, polystyrene

Table 1. Characterization of the SBS Samples

sample code	wt ratio (PS/R)	vol fraction of PS	total M_w (kg/mol)	M_w of the S block (kg/mol)	M_w/M_n
SBS-1	30/70	0.27	93	28	1.37
SBS-2	28/72	0.25	96	27	1.27
SBS-3	31/69	0.28	137	42	1.49
SBS-4	31/69	0.28	209	65	1.27
SBS-5	30/70	0.27	280	84	1.91

(TEM) is not, in general, sufficiently high for interface studies. Solid-state NMR offers another possible tool for high-resolution measurements of interface. Furthermore, because of the its generality, it can be used to study a much wider range of polymer materials than other methods.

The absence of any sample modification requirements is yet another significant advantage of this method. Because of this, it can be used to investigate the effect of processing conditions on the microdomain structure of polymers.

One of the primary disadvantages of the NMR method is that no morphological information is directly available. Furthermore, determination of the domain sizes from the spin diffusion experiment is dependent upon the morphological information. Small-angle X-ray scattering, as a complementary method, is an ideal tool for providing access to this type of data.

The dependence of the domain size information on simulation models must also be acknowledged as a potential obstacle. So far, a few of models have been developed to obtain various domain size parameters from the NMR measurements.[6,11−13] The spin diffusion process, which is measured by NMR experiments as mentioned before, can be numerically simulated by solving spin diffusion equations with proper initial and boundary conditions.

In this paper, the microphase structure and the interface of a few poly(styrene−butadiene−styrene) triblock copolymers are investigated. A combination of SAXS and NMR measurements allows us to evaluate the shape and the size of the domains as well as the thickness of the interface. This combined approach also allows us to examine the validity of the simulation model used for NMR analyses.

2. Experimental Section

2.1. Samples. The poly(styrene−butadiene−styrene) (SBS) samples are commercial triblock copolymers that were generously donated by the Shell Company. The polystyrene (PS) and polybutadiene (PB) homopolymers are supplied by Aldrich, and the polybutadiene rubber consists of about 90% 1,4-butadiene which is similar to the rubber component of the copolymer microstructure. The chemical structure of these samples is given in Scheme 1. The weight ratios of the polystyrene and the butadiene rubber, as determined by solution NMR and given in Table 1, are consistent with the data given in the Shell catalog. In this paper, the abbreviation SBS-n (n = 1, 2, ..., 5) will be used for the five samples. The molecular weights and polydispersities of these samples, as determined by GPC, are also listed in Table 1.

2.2. Sample Preparation. As mentioned in the Introduction, it is not necessary to make extensive sample modification for NMR measurements. However, to compare the results from solid-state NMR and SAXS methods, films were made and used for both NMR and SAXS measurements. The film specimens were obtained from a toluene solution of about 5 wt % polymer concentration by evaporating the solvent slowly at room temperature for a week. To further remove the toluene, the films were vacuum-dried at room temperature for about 4 days.[14,15] For the NMR measurement, the samples were prepared by cutting the film into about 2−3 mm^2 small pieces.

2.3. SAXS Measurements. Small-angle X-ray scattering (SAXS) measurements were made using both in-house and synchrotron facilities. The in-house data were obtained using a Cu X-ray tube with a similar setup as described in our previous publications.[16,17] The results from the in-house data were used to calibrate the synchrotron data through comparison of the scattering profiles from identical samples.

The Brazilian synchrotron SAXS facility is described in the paper by Kellermann et al.[18] All of the measurements were made using a Kodak SO-230 image plate with a spatial resolution of 218 μm at a wavelength of 1.608 Å (6.9 keV). A sample-to-detector distance of 1256.5 mm was used for all of the relevant data. The minimum accessible angle, as seen in the analysis plots provided, is about 0.07 Å^{-1}.

The image plate is a 2-dimensional detector. Preliminary 2-D scattering profiles are reduced to 1-D data using the X-ray program, Version 1.0 (1996), Université Mons Hainaut, for further analysis. Sector integration is done assuming a 100 μm pixel width and integrating over an arc width of either 25° (for the short or x range of data with the highest signal-to-noise ratio) or of 9.0° (for the longer angular range).

2.4. NMR Measurements. All NMR measurements were made on a Bruker ASX-200 spectrometer, operating at 200 and 50.29 MHz for ^{1}H and ^{13}C, respectively. The ^{13}C spectra were obtained using cross-polarization and magic angle spinning techniques. The optimum contact time used for all the ^{13}C spectra is 1 ms, and all the spectra were obtained at room temperature (about 19 °C).

^{1}H spin−lattice relaxation times were measured using an inversion−recovery pulse sequence through cross-polarization to ^{13}C. Spin diffusion measurements were carried out with ^{13}C detection through cross-polarization using a dipolar filter pulse sequence.[19] The selection of the mobile component was achieved by five repeating cycles with a 9 μs delay time. Phase cycling (PC, an alternation of a π pulse or no pulse) was used after the selection in the measurements.

3. Results and Discussions

3.1. Morphology Information. As mentioned earlier, the shape and sizes of the microdomains are very important to many use properties exhibited by the materials. The theory of the microphase separation has been first provided by the work of Helfand and Wassermann.[20,21] They described the microphase separation as an equilibrium of several factors; the interaction between A and B segments is repulsive and therefore gives a driving force for domain growth so as to reduce the surface-to-volume ratio. The equilibrium morphology of the domains, size and shape, should be determined by a balance of surface-to-volume ratio, loss of conformational entropy, and repulsive segment interaction. It has been found, especially by electron microscopy, that the dispersed microphases can be, in general, three-dimensional spheres, two-dimensional cylinders, or one-dimensional lamellae. However, ^{1}H spin diffusion measurements cannot provide us such information directly. Furthermore, the determination of domain sizes by ^{1}H spin diffusion measurements is dependent upon the morphological information on the probed materials.

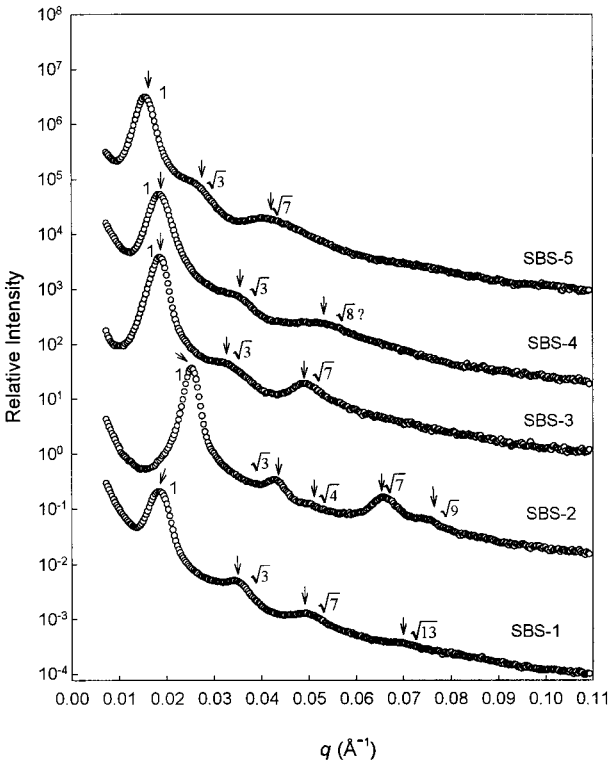

Figure 1. Synchrotron SAXS scattering intensity distribution as a function of scattering angle for the SBS samples.

SAXS Studies. Synchrotron SAXS studies for all five samples have been performed, and the reasonably high electron density contrast makes it possible to examine the phase behavior of all the triblock copolymers. The synchrotron scattering patterns of the SBS series samples exhibit multiple interaction peaks and the relative intensities as a function of q for all the SBS samples are given in Figure 1. The momentum transfer, q, is defined as $q_{max} = (4\pi/\lambda) \sin \theta$, where 2θ is the scattering angle and λ is the wavelength. From the SAXS profile shown in Figure 1, it can be seen that, in general, the peak positions have a relation of 1, $\sqrt{3}$, $\sqrt{4}$, $\sqrt{7}$, and $\sqrt{9}$ for all samples except for SBS-4. This is typical for d-spacings of hexagonally packed cylinders with sufficiently long-range order,[14,22] and the results are consistent with previous studies by Keller et al.[23,24] and Lewis and Price.[25−27] For the SBS-4 sample, it seems that there is a scattering peak at a relative q value of $\sqrt{8}$ instead of $\sqrt{7}$, and the reason for this is not yet clear. No conclusions regarding the actual domain shapes can be made by this analysis. On the basis of the volume fraction of this material in Table 1, we may assume cylindrical polystyrene domains with hexagonal packing in the polybutadiene matrix. As is well-known, unlike electron microscopy which can easily visualize the two types of blocks if one of them is stained, X-ray diffraction cannot distinguish the chemical nature of the different blocks and to identify which blocks form the cylinders and the matrix. For our SBS systems, it is evident that the cylindrical polystyrene domains are hexagonally arranged in polybutadiene rubber matrix based on the large volume fraction difference between the two blocks in all five samples.

3.2. Domain Size Information. SAXS Studies. The observed first-order maximum for all five samples in Figure 1 can be interpreted as a result of interparticle distances, and the calculated domain spacings are give in Table 2. This is obtained using the relation[28]

$$d_L(\text{SAXS}) = (4/3)^{1/2} d = 1.15d, \quad \text{where } d = 2\pi/q_{max} \tag{1}$$

Here d is the plane spacing associated with the first Bragg peak for a hexagonally ordered system and d_L (NMR) is the interdomain distance. To further confirm our results, analysis of desmeared scattering in-house data from identical samples was also done, and the calculated results for the interdomain distances are in very good agreement with those results obtained from synchrotron data given in Table 2.

Table 2. Microdomain Structure Results from SAXS Studies

sample code	$q_{max} \pm$ 0.005 nm	d_L[a] (nm) ± 2 nm	R_g[b] (nm)	d_{PS}[c] (nm) ± 2 nm	d_I[d] (nm)
SBS-1	0.185	39	5.1 ± 0.5	14	1.6 ± 0.3
SBS-2	0.240	30			1.1 ± 0.3
SBS-3	0.190	38	4.3 ± 0.4	12	2.1 ± 0.3
SBS-4	0.187	39	5.2 ± 0.4	15	0.9 ± 0.3
SBS-5	0.150	48	4.6 ± 0.5	13	1.4 ± 0.4

[a] d_L is the distance between the polystyrene domains. [b] R_g is the radius gyration of the polystyrene domains. [c] d_{PS} is the diameter of the polystyrene domains. [d] d_I is the interfacial thickness.

Since there is no clear evidence of single particle scattering, estimation of polystyrene particle sizes from Figure 1 is not attempted. Feigin et al.[29] have discussed Guinier analysis and shown that a linear relation should be observed at sufficiently small angles with a slope of $-R_g^2/3$ for 3-dimensional globular particles where the useful angular range is generally limited to values of q with $qR_g < 1$. A Guinier plot in the form of ln(intensity) vs q^2 (q = momentum transfer) was attempted in order to estimate the radius of gyration, R_g, of the scattering particle, and a significant linear region was found for the SBS-1, SBS-2, and SBS-4 samples. The radii of gyration of about 26.1 nm for SBS-1, 27.5 nm for SBS-2, and 23.8 nm for SBS-4 samples were found from the analysis of these linear regions. No clear linear regions have been found for the SBS-3 and SBS-5 samples due to the presence of interaction structure and estimation of the polystyrene particle sizes for these two samples are not made. The linearity of the Guinier plots can be interpreted as a partial confirmation of the 3-dimensional structure of the microdomains. However, no definite conclusions can be made regarding the true nature of the particle anisometry by this analysis. In fact, Guinier analysis was also attempted assuming rodlike shapes since the SAXS scattering pattern indicates a hexagonal structure, implying a cylindrical morphology[14,22] for all samples except for SBS-4. However, no significant improvement over the 3-D Guinier analysis could be determined. This result probably can be explained as due to the limited length of the cylinder in relation to its diameter, meaning that it is still essentially a 3-dimensional particle. It is very reasonable to assume that the shape of the particles is ellipsoidal given the volume fraction[30,31] and multiple Bragg peaks of the SAXS data profile. For a 3-dimensional ellipsoidal particle shape, the radius of gyration of the particle obtained by a Guinier plot is actually an average of the length of the elongated axis and the cross-sectional dimension.[29] Assuming that the length of the elongated axis is much longer than the length of the

cross-sectional axis, the radius of gyration of the particles obtained in this way will be much larger than the radius associated with the cylinder model. In this case, using Guinier analysis to estimate the sizes of single particles is no longer appropriate.

Particle size estimates were made through indirect transform analysis[32] of the high-q scattering data (after interaction structures) from the SBS samples. The indirect transform analysis was performed using the program GNOM[33] which allows one to choose between several general structural models for analyzing SAXS data from a dilute systems. A monodisperse system of rodlike particle model was chosen to fit the synchrotron data at values of q excluding the interaction peaks. In all cases, this model gave "reasonable" fits to the truncated data, and the estimated values for radii of gyration using this approach are about 5.1 nm for the SBS-1, 4.3 nm for SBS-3, 5.2 nm for SBS-4, and 4.6 nm for SBS-5 samples. These values can be used to provide rough estimates of the cross sections (assumed circular) of the rods by multiplying a factor of $\sqrt{2}$.[29] The obtained particle sizes for the SBS-1, SBS-3, SBS-4, and SBS-5 are summarized in Table 2. No information is available for the SBS-2 sample since it would require far too much deletion of low-q information to permit a reasonable interpretation of the data. The indirect transform method of small-angle scattering data treatment is relatively insensitive to low-q information and also provides a measure of the pair distribution function, $P(r)$, of the scattering objects. No insight into the shape of the cross section was obtained from the $P(r)$ curves using rodlike model results given the relatively poor quality of the fit results with the truncated data.

Proton Spin−lattice Relaxation Time. The fact that proton spin−lattice relaxation time in the laboratory frame, T_1(H), and in the rotating frame, $T_{1\rho}$(H), can be used to semiquantitatively estimate the microstructure of heterogeneous system has been previously demonstrated by many authors.[34,35] Each parameter gives information on the sizes of domains at different levels. Separate $T_{1\rho}$(H)'s and T_1(H)'s have often been used as proof for lack of miscibility, and the actual values can be used to estimate upper and/or lower limits of domain sizes.

In Figure 2, ^{13}C CP/MAS spectra of the PB, PS, and SBS-3 are shown. By comparison, it is easy to assign each peak for the SBS-3 spectrum. For each resolved signal and the spinning sideband of the protonated aromatic carbons of the PS peak in the SBS spectrum, T_1(H) values were measured, and the results are summarized in Table 3. The T_1(H)'s of polystyrene and rubber homopolymers of comparable molecular weights were also measured and are 1600 and 260 ms, respectively. These values are taken as the respective intrinsic T_1(H)'s for the polystyrene and the rubber in the copolymer. From Table 3, it can be seen that separate T_1(H)'s are obtained for all five samples, and this indicates the phase separation for all the studied materials. It is evident that spin diffusion causes a partial averaging of the two T_1(H)'s for all the observed copolymers in the Table 3. This implies that spin diffusion and spin−lattice relaxation occur at comparable rates in these systems, and the existence of different spin-relaxation times in the materials will affect the spin diffusion process.[13]

Spin Diffusion Experiments. Solid-state NMR of ^{1}H spin diffusion measurements has been used to quantitatively extract the microdomain structures of polymer materials.[3−7,9,10] The mobility difference between the rigid polystyrene and the mobile polybutadiene rubber allows us to apply a dipolar filter pulse sequence to obtain the spin diffusion measurements. The dipolar filter pulse sequence[19] contains 12 $\pi/2$ pulses separated by a delay time t_d. If a relatively long delay time is used and the cycles are repeated for a few times, the rigid component decays faster than the mobile component, and it cannot be refocused by the pulse sequence in the end. The proton magnetization of the mobile component will be selected as the magnetization source. During the following mixing time, the protons in the rigid component will gain magnetization from the protons in the mobile component through spin diffusion. To identify different protons and get a high-resolution spectrum, the spectra were recorded through ^{13}C detection.

In Figure 3, a series of spectra of the SBS-3 sample at different mixing times are shown. It can be seen from the spectrum taken at the shortest mixing time (500 μs) that only the magnetization of the mobile polybutadiene is present, and the magnetization of the polystyrene component has been eliminated by the dipolar filter pulse sequence. With the increase of mixing time, the polystyrene magnetization appears and increases. After the complete recovery of the polystyrene magnetization, the intensity of all the peaks is reduced. This decrease is directly related to the phase cycling used in the spin diffusion measurements. As discussed in the literature,[36] spin−lattice relaxation leads to magnetization

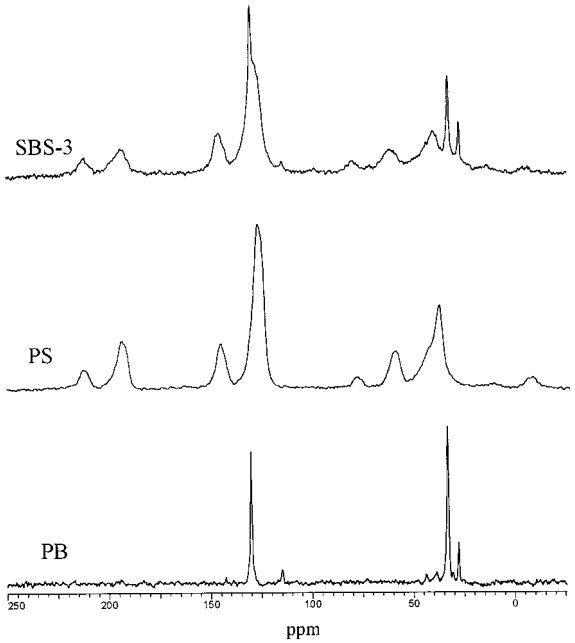

Figure 2. ^{13}C CP/MAS NMR spectra of the PS, PB, and SBS-3 samples.

Table 3. T_1(H) Values for the PB and PS in the SBS Samples

sample code	T_1 of the PS block (ms)	T_1 of the PB block (ms)
SBS-1	515 ± 10	360 ± 20
SBS-2	448 ± 20	385 ± 20
SBS-3	470 ± 30	300 ± 10
SBS-4	508 ± 60	312 ± 15
SBS-5	471 ± 30	346 ± 20
PS	1600 ± 100	
PB		260 ± 20

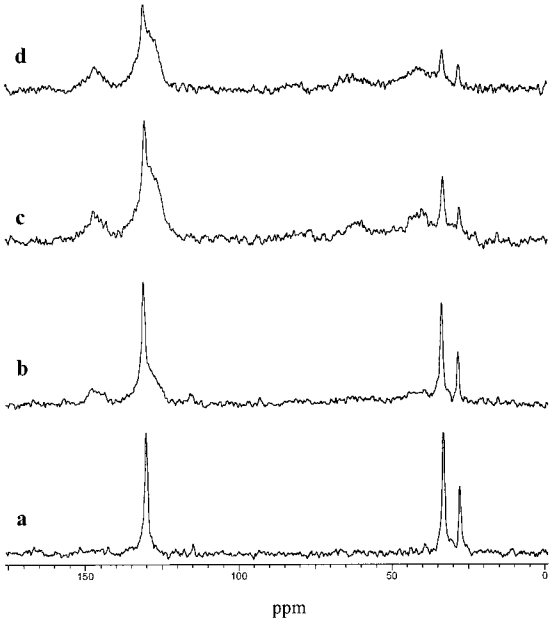

Figure 3. Dipolar filter spectra of the SBS-3 sample at different mixing time: (a) 500 μs, (b) 5 ms, (c) 150 ms, and (d) 400 ms.

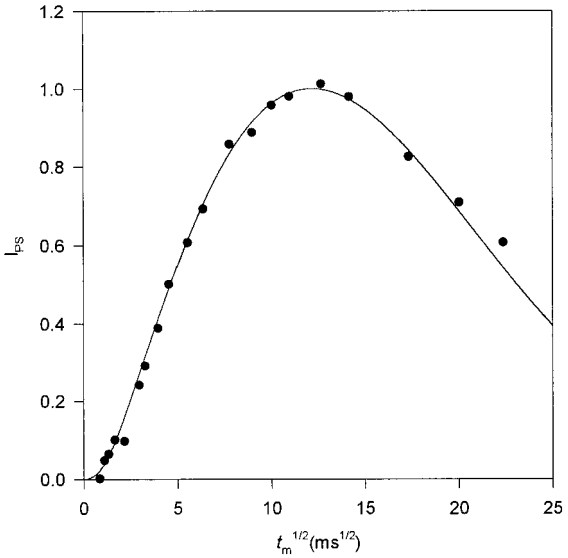

Figure 4. Magnetization growth of the protonated aromatic carbons of polystyrene for SBS-3 sample as a function of mixing time using the dipolar filter method. The solid dots are experimental data. The fitting parameters are the polystyrene domain d_{PS} = 18 nm, interface d_I = 2 nm, and long period d_L = 39 nm.

contributions that cannot be distinguished from that of spin diffusion. Its effect can be reduced by a simple alternation of a π pulse and no pulse before the mixing time. If the selected proton magnetization is aligned along $+z$ and $-z$ axes in alternating scans, most of the T_1(H) relaxation contributions are canceled. The application of phase cycling causes all of the observed signals to decrease in intensity at long mixing times. The reduction in the measured signal intensity is corrected by $\exp(t_m/T_1)$, where t_m is the mixing time and T_1 is the proton spin−lattice relaxation time for the resonance being measured. Quantitative analysis of spin diffusion curves with the measured signal intensity being corrected in the experiment by use of phase alternation has been previously reported.[7,8,13,36] However, such data correction based on exponential multiplication for a heterogeneous system with different intrinsic T_1(H)'s in the two regions sufficiently corrects the spin−lattice relaxation effect only when the two intrinsic spin−lattice relaxation times are longer than the time needed to reach the spin diffusion equilibrium, as discussed by Friebel et al.[37] It is not necessary to correct the raw spin diffusion data if the T_1(H) effect is explicitly treated in the simulation of the spin diffusion, as discussed in previous literature.[9,11,13] The magnetization recovery of the polystyrene at different mixing time for the SBS-3 sample without T_1(H) correction is shown in Figure 4. Since there is a chemical shift overlap of polystyrene and polybutadiene peaks at about 127 ppm in the ^{13}C spectrum, the magnetization of the polystyrene at different mixing times was obtained by subtracting a factor from the total integral of this peak.

$$I_{PS} = I_{127} - f\, I_{33} \tag{2}$$

Here I_{127} and I_{33} are the integrals of the carbon resonance at 127 ppm and the peak at 33 ppm, respectively, and f is the integral ratio of I_{127}/I_{33} from the dipolar filter spectrum without a mixing time.

Simulations of the Spin Diffusion Curves. As discussed above, the magnetization recovery of the initially suppressed component as a function of mixing time contains information about domain sizes. However, a quantitative determination of the domain size requires numerical simulation of the spin diffusion curves.

The simulation model of spin diffusion, including the T_1(H) spin−lattice relaxation effect, used in this work has been described in detail by Wang et al.[13] and used to extract microdomain structure information in two polymer systems.[9,17] The combined spin diffusion and spin−lattice relaxation is described by the following diffusion equation:

$$\frac{\partial c_z^A(r,t_m)}{\partial t_m} = D_A \Delta c_z^A(r,t_m) + \frac{c_z^\infty - c_z^A(r,t_m)}{T_{1A}} \tag{3}$$

where $c_z^A(r,t_m)$ is the specific spin magnetization, D_A is the spin diffusion coefficient, and T_{1A} is the intrinsic spin−lattice relaxation time in phase A. c_z^∞ is the equilibrium value of the specific spin magnetization in the system. A similar equation exists for the B phase. The above two equations should be solved with proper initial and boundary conditions as outlined by Wang in a previous publication.[12] The total spin magnetization in each phase, which is proportional to the NMR signal intensity, can be conveniently obtained by integrating the specific spin magnetization over the corresponding regions, Ω_A or Ω_B; i.e.,

$$M_Z^A(t) = \rho_H^A \int_{\Omega_A} C_Z^A(r,t)\, dr \tag{4}$$

where ρ_H^A is the proton concentration in the phase A. Simulated spin diffusion curves were obtained by plotting the total spin magnetization in the PS domain as a function of $\sqrt{t_m}$.

A system with an interface in which the chemical composition gradually changes across the phase boundaries is considered in the simulation model, and such a system can be divided into three regions: source, sink, and interface. We further assume that linear changes

Table 4. Some Parameters for the Two Components in the SBS Samples

phase	proton fraction	density, g/cm^3	proton density, g/cm^3	diffusion coeff, nm^2/ms	T_1 relaxation, ms
PS	0.077	1.060	0.081	0.80	1600
PB	0.111	0.900	0.100	0.05	260

of the spin diffusion coefficient, proton concentration, and intrinsic proton spin−lattice relaxation rate occur across the interfacial region and that the linear change of intrinsic relaxation rate can be written as

$$\frac{1}{T} = \frac{1}{T_{1A}} + \frac{1 - f_A}{T_{1B}} \tag{5}$$

where f_A is the composition fraction of A component.

It can be seen from eq 3 that the spin diffusion coefficient, D, is an important parameter in the numerical simulation. Therefore, knowledge of the spin diffusion coefficient is a prerequisite for accurately characterizing the domain sizes. There are relatively few discussions about the spin diffusion coefficient in the literature,[6,38] and many unknowns remain in this area. In this work, spin diffusion coefficient values of 0.8 nm^2/ms for the PS and 0.05 nm^2/ms for polybutadiene have been used to perform the simulations.[6,38]

It also can be seen from eq 3 that solutions for the diffusion process will depend on dimensionality or morphology of the materials. However, it is difficult for NMR itself to provide such information. SAXS is a very good method for morphology studies, as discussed in section 3.1. For all five samples, a dimensionality of 2, cylindrical polystyrene domains arranged in a polybutadiene matrix as suggested by SAXS studies, was used for all of the simulations. All other information used in the simulations is given in Table 4.

As discussed in a previous paper,[17] although a cylindrical domain arrangement in a hexagonal lattice is thought to better describe the true morphology of the materials, there are a few reasons that make it difficult to use such a model to simulate the spin diffusion curves. For simulation simplicity, we assume that a rectangular parallelepiped with a square base in a two-dimensional simple square lattice arrangement is formed in the rubber matrix. Such a model will introduce two main errors in the results.[17] One is in the domain sizes of the dispersed phase which will be underestimated by about 13% with the model assuming a square base instead of a circle base cylinder domain. The other error is in the interdomain distance, which is underestimated by about 7% by assuming a two-dimensional simple square lattice instead of the more accurate hexagonal lattice.[17] Details about the model and the possible errors introduced by it were discussed in a previous publication.[17]

The initial slower increase of intensity in the spin diffusion curve (Figure 4) may suggest the presence of a small interface between the polystyrene and the rubber phases.[3,12,19] Therefore, in our model, the microphase structure of the sample is assumed to consist of a polystyrene square, surrounded by an interface, and then a continuous rubber phase. The area of each square represents the volume fraction of the corresponding domain. For a given set of microphase structure parameters, two separate simulations with different initial conditions were performed. The first one corresponds to the process in which the data are collected immediately after the dipolar filter pulse, and the initial magnetization for the source and sink are 1 and 0, respectively. The second one is related to the data collecting process after a π pulse and the initial magnetization of the source and sink are −1 and 0, respectively. The difference of magnetization in the PS (or rubber) region from the above two simulations is directly comparable with the experimental data obtained using phase alternation. To obtain the microstructure of the samples, the domain size of PS, d_{PS}, and the interfacial thickness, d_I, have been changed independently to fit the spin diffusion curve. It has been found that the spin diffusion curve is sensitive to the various domain size parameters. The best fitting parameters obtained for SBS samples are summarized in Table 5. The uncertainties in each parameter in Table 5 are estimated from the fitting process only. Domain size parameters chosen outside of the uncertainty range give a poor fitting. For example, if the domain size value of the dispersed polystyrene is chosen to be $d_{PS} = 16$ nm or $d_{PS} = 20$ nm (outside of $d_{PS} = 18 \pm 1$ nm), there are visible differences in the magnetization growth curves when compared to the experimental curve. The best fitting curve for the SBS-3 sample is shown as a solid curve in Figure 4 with the inner polystyrene domain size, $d_{PS} = 18$ nm, and the interface, $d_I = 2$ nm. The long period, the distance between two adjacent polystyrene squares, is $d_L = d_{PS} + 2d_I + d_R = 39$ nm. The agreement between experiment and simulation is quite good for all of the copolymers. The simulations using the model including the effects of ^{1}H spin−lattice relaxation capture the basic feature of the spin diffusion curves, that is, the sigmoidal shape of the experiment. The signal of polystyrene increases slowly at the beginning and reaches the maximum at $t_m^{1/2} \approx 12.5$ ms$^{1/2}$ and then decays because of proton T_1 effects.

Table 5. Microdomain Structure Results from NMR Techniques

sample	d_{PS} (nm) ± 1 nm	d_I (nm) ± 0.5 nm	d_L[a] (nm) ± 3 nm
SBS-1	15	2.0	33
SBS-2	14	2.0	32
SBS-3	18	2.0	39
SBS-4	17	2.0	37
SBS-5	20	2.0	42

[a] d_L (long period) = d_{PS} (polystyrene) + $2d_I$ (interface) + d_B (polybutadiene).

For comparison, the microdomain structure results obtained from NMR and SAXS are given in Table 6. It can be seen that the interdomain distances obtained from the two methods are in good agreement and generally increase with the increase of the total molecular weight. The domain sizes of polystyrene obtained from NMR measurements generally increase with the increase of the molecular weight of the styrene blocks. These results are consistent with the prediction of equilibrium theory.[21] However, there are some discrepancies for some samples regarding the domain sizes of polystyrene phase obtained from NMR simulation and SAXS indirect transform methods. These discrepancies may be mainly or at least partially caused by the limited quality of scattering data after excluding the interaction peaks. This example further demonstrates that SAXS and NMR methods complement each other, and the combined approach greatly increase the reliability of the findings.

3.3. Interface Information. Porod Analysis. As mentioned in the Introduction, SAXS and SANS have

Table 6. Comparison of the Results from NMR and SAXS

sample code	d_L (nm) (NMR) ± 3	d_L (nm) (SAXS) ± 2	d_{PS} (nm) (NMR) ± 1	d_{PS} (nm) (SAXS) ± 2	d_I (nm) (NMR) ± 0.5	d_I (nm) (SAXS)	d_I (nm) (ref 43)
SBS-1	33	39	15	14	2.0	1.6 ± 0.3	
SBS-2	32	30	14		2.0	1.1 ± 0.3	2
SBS-3	39	38	18	12	2.0	2.1 ± 0.3	2
SBS-4	37	39	17	15	2.0	0.9 ± 0.3	
SBS-5	42	48	20	13	2.0	1.4 ± 0.4	

previously been the only useful methods for estimating the interfacial thickness and have been used by many authors in the literature.[15,39−41] In this section, the results of interfacial thickness obtained from Porod analysis will be discussed. Porod analysis is generally performed in the region of the final slope of the scattered intensity. The final slope of the scattering curve implies the high-q region of the small-angle scattering profile. The simple geometric arguments that can be found in the texts by Glatter and Kratky (1982)[42] and Feigin and Svergun (1987)[29] lead to the prediction that the (ideal) slope of the scattering goes as[39,40−42]

$$I(q) = \frac{Q}{\pi}\frac{S}{V}\frac{1}{q^4} \tag{6}$$

The invariant, Q, is a measure of the total scattering intensity. The parameter S is the total interfacial area of the particles while the volume V would be the total volume occupied by the particles. That is, the specific surface, S/V, can be obtained from the final slope of the scattering curve given a valid estimate of the invariant, Q. Porod analysis is generally done by plotting the data in the form of Iq^4 vs q^4 and obtaining a value of the constant at high q. This is, of course, the ideal case and very rarely seen in real materials. The derivation of the above expression is based on the simple model of completely uniform electron density within the distinct phases (i.e., particle and background) with an infinitely sharp boundary separating them. In real systems, there will always be some heterogeneity within the phases due to atomic structure as well as possible phase intermixing. If the heterogeneity occurs at sufficiently small length scales, the resulting scattering contribution may be represented as a constant in the small-angle region. That is,

$$I(q) = C_0 + \frac{P}{q^4}, \quad P = \frac{Q}{\pi}\frac{S}{V} \tag{7}$$

Then a plot of Iq^4 vs q^4 will yield a straight line of slope C_0 at high q.[29] Identification of a significant linear region at high q usually means that the dominant heterogeneity is, indeed, at significantly smaller length scales than the particle sizes, and the effect can be corrected. With the measured value of C_0 subtracted off from the original data to yield I_{corr}, a new plot of $I_{corr}q^4$ vs q^4 is generated. Assuming that the scattering background has been adequately removed, an estimation of P, the parameter containing details of the interface, can then be made. In the case of a finite interfacial thickness, the plot of $I_{corr}q^4$ vs q^4 will show a negative deviation from the ideal constant value at high q. The interfacial thickness can be estimated from this plot by assuming a convolution of the ideal electron density profile (sharp interfaces) with a Gaussian smoothing function of the form $\exp(-r^2/2\sigma^2)$, σ being the standard deviation and a measure of the interfacial thickness.

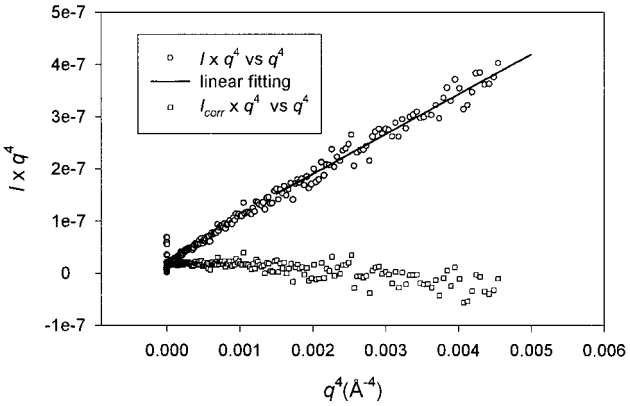

Figure 5. Porod plot in the form of Iq^4 as a function of q^4 for the SBS-1 sample.

With this simple model, the fully background-corrected scattering is predicted to have the form

$$I(q) = \frac{P}{q^4}\exp(-\sigma^2 q^2) \tag{8}$$

Given this form, a plot of $\ln(I_{corr}q^4)$ vs q^2 should show a linear region at high q with a slope of $-\sigma^2$. The interfacial thickness is then simply given by $(2\pi)^{1/2}\sigma$.

A plot in the form of Iq^4 vs q^4 was carried out for all five samples, and a linear region at high q was found in every case. In Figure 5, a typical plot of Iq^4 vs q^4 (circles) and a linear fitting at high-q region for SBS-1 sample are given. Initial determination of a constant, C_0, did not completely remove the high-q scattering background. A plot of $(I - C_0)q^4$ vs q^4 again showed a clear linear region of positive slope at somewhat lower q values. A new, corrected intensity is then obtained by subtracting the value of this slope from $(I - C_0)$. This scattering intensity is used for further analysis of the interface structure. Plots of $I_{corr}q^4$ vs q^4 were attempted for all samples, and a negative deviation was found in all cases. A sample plot of $I_{corr}q^4$ vs q^4 (squares) for the SBS-1 sample is also shown in Figure 5. Figure 6 shows a Porod plot in the form of $\ln(I_{corr}q^4)$ vs q^2 for the SBS-1 and the linear fit used for estimation of the interfacial thickness of this sample ($d_I = 1.6 \pm 0.4$ nm). In all cases, a region of negative slope, although very weak, is readily identified. All of the results pertaining to the interfacial thickness from Porod analysis are summarized in Table 2.

Simulation Model. Porod analysis from SAXS measurements is very efficient for extracting interface information and has been used for many years.[39,40] However, it should be noted that one of the biggest problems with this type of analysis is poor counting statistics at the relevant high-q regions. It is also impossible to proceed when the electron density heterogeneities leading to unwanted background scattering are sufficiently large to obscure any valid Porod regions corresponding to the homogeneous approximation.

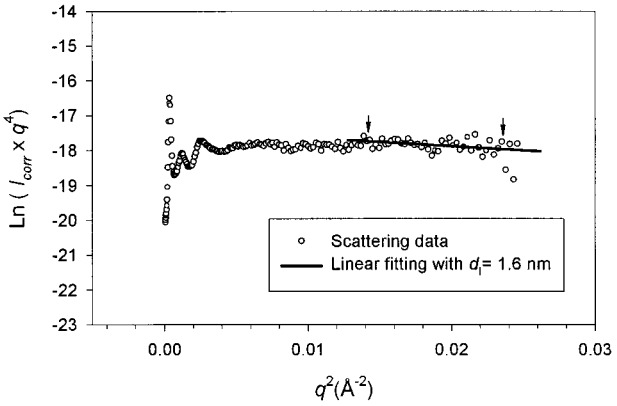

Figure 6. Porod plot after all background *correction* in the form of $\ln(I_{corr}q^4)$ as a function of q^2 for the SBS-1 sample.

The NMR method has been found to be a more direct approach to the study of interfacial structures than the small-angle X-ray scattering (SAXS) method.[43] The initial slower increase of intensity in the spin diffusion curve (Figure 4) suggests the presence of an interface.[3,12,19] However, estimation of this interfacial thickness must be performed through a simulation model. If the model is well defined for the description of the spin diffusion process, this is an efficient way to extract interfacial information. As discussed in section 3.2, interfacial thickness, d_I, is one of the independent fitting parameters used to fit the spin diffusion curve. The estimation of the interface thickness for the SBS samples was obtained using a simulation model including the T_1 effect, as described in section 3.2, and the results are given in Table 5. A 2 nm interfacial thickness was found for all of the SBS samples. These results are generally consistent with the SAXS results as well as with previous studies.[43] It is also found that our simulation model is very sensitive to the interfacial thickness. To illustrate this point, simulations with different interfacial thickness, d_{PS} = 18 nm, d_I = 1 nm, and d_{PS} = 18 nm, d_I = 3 nm, have been performed, and the results for the SBS-1 sample are given in Figure 7 as a dashed line and a solid line, respectively. It is obvious that there is a visible discrepancy for both fits. A relatively larger PS domain size parameter, for example, d_{PS} = 19 nm, d_I = 1 nm, and a relatively smaller PS domain size parameter, for example, d_{PS} = 17 nm, d_I = 3 nm, can be chosen to fit the experimental curve for a given interfacial thickness, d_I = 1 nm and d_I = 3 nm, respectively, However, a good fit cannot be obtained without changing the interfacial thickness parameter.

It can be seen from the above discussion that Porod analysis is a powerful method for interface analysis but that poor counting statistics at high q as well as significant heterogeneity region may preclude quantitative estimation of interfacial thickness in some applications. The more direct and simplest approach to quantitatively estimate interfacial thickness is the spin diffusion simulation, which is itself dependent on the validity of the simulation model.

The validity of our simulation model that includes the spin−lattice relaxation effect has been previously demonstrated, and the results obtained using this simulation model including the T_1 effect are more accurate than those obtained using the pure spin diffusion model.[13,9,17] In this case, the spin diffusion experimental data (solid dots) for the SBS-4 sample and the simulated curves made by both models are given in Figure 8. Since

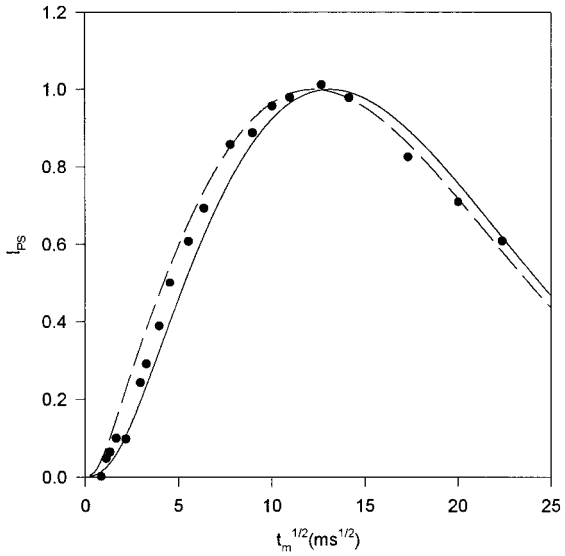

Figure 7. Magnetization growth of the protonated aromatic carbons of polystyrene for SBS-3 sample as a function of mixing time using the dipolar filter method. The solid dots are experimental data. The fitting parameters are the polystyrene domain d_{PS} = 18 nm, interface d_I = 1 nm for the dashed line, and the polystyrene domain d_{PS} = 18 nm, interface d_I = 3 nm for the solid line.

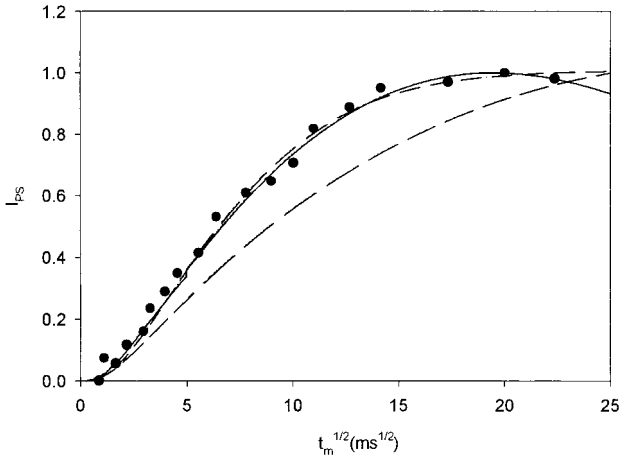

Figure 8. *Corrected* magnetization growth of the protonated aromatic carbons of polystyrene for SBS-4 sample as a function of mixing time using the dipolar filter method. The solid dots are experimental data after multiplication a factor of exp(t_m/T_1). Details are in the text. The solid line is fitting curve obtained using a model that considers the T_1 effect with the polystyrene domain d_{PS} = 17 nm, the interface d_I = 2 nm, d_L= 37 nm. The dashed line is the fitting curve obtained using a pure spin diffusion model with the same parameters as above. The dash−dot line is the best fitting curve obtained using a pure spin diffusion model with the polystyrene domain d_{PS} = 9 nm, interface d_I = 3 nm and d_L = 23 nm.

the previous model without the proton T_1 effect will be used to simulate the spin diffusion experiment, the raw spin diffusion data for SBS-4 sample have been *corrected* by multiplying a factor of exp(t_m/T_1), as described in the literature.[6−8,36] T_1 is the spin−lattice relaxation time for the PS component in the SBS-4 copolymer given in Table 3. The domain size parameters for SBS-4 in Table 5 (d_{PS} = 17 nm, d_I = 2 nm, d_L= 37 nm), obtained by simulating the raw spin diffusion data using a model that includes the T_1 spin−lattice relaxation effect, were used to simulate the *corrected* spin diffusion data, and the results are shown in Figure 8 as a solid line. It can

be seen that the agreement between the experimental data and the simulated data is reasonably good, which in reverse illustrates that the raw spin diffusion data and the *corrected* spin diffusion data contain the same information on the domain sizes of the material. The *correction* of raw spin diffusion data is not necessary if the simulations were made using a model that considers the proton spin−lattice relaxation effect. A simulation using the pure spin diffusion model[12] with the same domain size parameters was also made, and the result is shown in Figure 8 as a dashed line. It is evident that a large discrepancy exists for using a pure spin diffusion model, without considering the proton spin−lattice relaxation effect. It can be seen that the simulated curve obtained by the pure spin diffusion model[12] predicts a much slower magnetization recovery than that of experiment. To fit the experimental data, a smaller domain size for the PS and a slightly larger interfacial thickness parameter have been used to fit the data, and the best fitting curve obtained using this pure spin diffusion model is given in Figure 8 as a dash−dot line with the domain size parameters, $d_{PS} = 9$ nm, $d_I = 3$ nm, and $d_L = 23$ nm. In comparison with the results from SAXS studies given in Table 6 and previous studies in the literature,[43] a value of 3 nm interfacial thickness suggested by the simulation using the pure spin diffusion model[12] seems slightly large but still reasonable. However, the long period of 23 nm (interdomain distance) is much smaller than the value suggested by SAXS (39 nm in Table 6). On the other hand, the interdomain distance of 37 nm in Table 6 obtained using the simulation model which considers the spin diffusion effect agrees very well with the result of 39 nm in Table 6 obtained from SAXS. In Figure 8 it is also evident that only the simulation model which includes the effects of the spin−lattice relaxation reproduces the decrease of the magnetization after a maximum point, which agrees with the experimental results for the SBS samples. This phenomenon has been found for other polymer systems[13,9,17] and indicates that the microdomain structure parameters obtained using a simulation model that includes the T_1 effects may be more accurate than those obtained using a pure spin diffusion model.

4. Conclusions

A combination of SAXS and solid-state NMR techniques has been used to investigate the microdomain structure of a series of SBS block copolymers. The multiple long-range order peaks in the SAXS data profiles indicate that majority of the studied SBS systems has a cylindrical morphology with hexagonal packing, and these results are consistent with previous reports. The microdomain structure parameters were obtained by simulating proton spin diffusion experiments with a model that considers spin−lattice relaxation effects. It was found that the quality of the simulations using a model that includes the T_1 term is very good for all of the materials. The interdomain distances obtained from solid-state NMR agree well with those obtained from SAXS. The simulation of the spin diffusion experiments indicates that the interfacial thickness is 2 nm for all SBS samples, and these results are generally in very good agreement with the results obtained from both Porod analysis and previous T_2 spin−spin relaxation studies.[43]

There are some discrepancies regarding the domain sizes of polystyrene between the SAXS indirect transform and NMR simulation. These discrepancies may be mainly or at least partially caused by the limited quality of the scattering data after excluding the interaction peaks in the indirect transform SAXS analysis.

Acknowledgment. We thank the Natural Science and Engineering Research Council (NSERC) of Canada and the Environmental Science and Technology Alliance of Canada (ESTAC) for their financial support. We also thank Ms. Rebecca Fraser for assistance with the in-house SAXS measurements and the National Synchrotron Light Laboratory (LNLS) in Brazil for assistance with the synchrotron SAXS measurements.

References and Notes

(1) VanderHart, D. L.; Manley, R. S. J.; Barnes, J. D. *Macromolecules* **1994**, *27*, 2826.
(2) VanderHart, D. L. *Macromolecules* **1994**, *27*, 2837.
(3) VanderHart, D. L. McFadden, G. B. *Solid-State NMR* **1996**, *7*, 45.
(4) Cho, G.; Natansohn, A. *Chem. Mater.* **1996**, *9*, 148.
(5) Jack, K. S.; Natansohn, A.; Wang, J.; Favis, B. D.; Cigana, P. *Chem. Mater.* **1998**, *10*, 1031.
(6) Clauss, J.; Schmidt-Rohr, K.; Spiess, H. W. *Acta Polym.* **1993**, *44*, 1.
(7) Cai, W. Z.; Schmidt-Rohr, K.; Egger, N.; Gerharz, B.; Spiess, H. W. *Polymer* **1993**, *34*, 267.
(8) Cho, G.; Natansohn, A.; Ho, T.; Wynne, K. J. *Macromolecules* **1996**, *29*, 2563.
(9) Jack, K. S.; Wang, J.; Natansohn, A.; Register, R. A. *Macromolecules* **1998**, *31*, 3282.
(10) Schmidt-Rohr, K.; Clauss, J.; Blümich, B.; Spiess, H. W. *Magn. Reson. Chem.* **1990**, *28*, S3.
(11) Kenwright, A. M.; Say, B. J. *Solid State NMR* **1996**, *7*, 85.
(12) Wang, J. *J. Chem. Phys.* **1996**, *104*, 4850.
(13) Wang, J.; Jack, K. S.; Natansohn, A. *J. Chem. Phys.* **1997**, *107*, 1016.
(14) Sakurai, S.; Kawada, H.; Hashimoto, T. *Macromolecules* **1993,** *26*, 5796.
(15) Todo, A.; Hashimoto, T.; Kawai, H. *J. Appl. Crystallogr.* **1978**, *11*, 558.
(16) Singh, M. A.; Ghosh, S. S.; Shannon, R. F. *J. Appl. Crystallogr.* **1993**, *26*, 787.
(17) Yu, H.; Wang, J.; Natansohn, A.; Singh, M. A. *Macromolecules* **1999**, *32*, 4365.
(18) Kellermann, G.; Vicentin, F.; Tamura, E.; Rocha, M.; Tolentino, H.; Barbosa, A.; Craievich, A.; Torriani, I. *J. Appl. Crystallogr.* **1997**, *30*, 880.
(19) Egger, N.; Schmidt-Rohr, K.; Blümich, B.; Domke, W. D.; Stapp, B. J. *Appl. Polym. Sci.* **1992**, *44*, 289.
(20) Helfand, E. *Macromolecules* **1975**, *8*, 552.
(21) Helfand, E.; Wasserman, Z. R. *Macromolecules* **1978**, *11*, 960.
(22) Winter, H. H.; Scott, D. B.; Gronski, W.; Okamoto, S.; Hashimoto, T. *Macromolecules* **1993**, *26*, 7236.
(23) Keller, A.; Pedemonte, E.; Wilmouth, F. *Nature* **1970**, *225*, 538.
(24) Keller, A.; Pedemonte, E.; Wilmouth, F. *Kolloid Z. Z. Polym.* **1970**, *238*, 365.
(25) Lewis, P.; Price, C. *Polymer* **1972**, *13*, 20.
(26) Lewis, P.; Price, C. *Nature* **1969**, *223*, 494.
(27) Lally, T.; Price, C. *Polymer* **1974**, *15*, 326.
(28) Sakurai, S.; Kawada, H.; Hashimoto, T. *Macromolecules* **1993,** *26*, 5796.
(29) Feigin, L. A.; Svergun, D. I. In *Structure Analysis by Small-Angle X-ray and Neutron Scattering*; Plenum Press: New York, 1987.
(30) Quirk, R. P.; Fetters, L. J. In *Comprehensive Polymer Science*; Allen, G., Ed.; Pergamon Press: Oxford; 1989**;** Vol. 7.
(31) Riess, G.; Hurtrez, G.; Bahadur, P. In *Encyclopedia of Polymer Science and Engineering*; Mark, H. F., Bikales, N. M., Overberger, C. G., Menges, G., Eds.; John Wiley & Sons: New York, 1985; Vol. 2.
(32) Svergun, D. I. *J. Appl. Crystallogr.* **1992**, *25*, 495.
(33) Svergun, D.; Semenyuk, A. *Small-Angle Scattering Data Processing by Means of the Regularization Techniques*; Institute of Crystallography, Academy of Sciences of Russia, 117333 Leninsky Pr., 59 Moscow, Russia, Version E4.2, 1993.
(34) Havens, J. R.; VanderHart, D. L. *Macromolecules* **1985**, *18*, 1663.

(35) McBriety, V. J. In *Comprehensive Polymer Science*; Allen, G., Ed.; Oxford, 1989; Vol. 1, p 397.
(36) Schmidt-Rohr, K.; Spiess, H. W. In *Multidimensional Solid State NMR and Polymers*; Academic Press: London, 1994.
(37) Friebel, S.; Harris, R. K.; Kenwright, A. M. *Magn. Reson.* **1997**, *35*, 29.
(38) Spiegel, S.; Schmidt-Rohr, K.; Boeffel, C.; Spiess, H. W. *Polymer* **1993**, *34*, 4566.
(39) Ruland, W. *Macromolecules* **1987**, *20*, 87.
(40) Jung, W. G.; Fischer, E. W. *Makromol. Chem. Makromol. Symp.* **1988**, *16*, 281.
(41) Annighöfer, F.; Gronski, W. *Makromol. Chem.* **1984**, *185*, 2213.
(42) Glatter, O.; Kratky, O. In *Small-Angle X-ray Scattering*; Academic Press: London, 1982.
(43) Tanaka, H.; Nishi, T. *J. Chem. Phys.* **1985**, *82*, 4326.

MA9910585